Science Signaling
AAAS

www.sciencesignaling.org/cgi/content/full/4/163/ra14/DC1

Supplementary Materials for

Vav1-Mediated Scaffolding Interactions Stabilize SLP-76 Microclusters and Contribute to Antigen-Dependent T Cell Responses

Nicholas R. Sylvain, Ken Nguyen, Stephen C. Bunnell*

*To whom correspondence should be addressed. E-mail: stephen.bunnell@tufts.edu

Published 8 March 2011, *Sci. Signal.* **4**, ra14 (2011)
DOI: 10.1126/scisignal.2001178

This PDF file includes:

Other Supplementary Material for this manuscript includes the following:
(available at www.sciencesignaling.org/cgi/content/full/4/163/ra14/DC1)

Movies S1 to S16 (.avi format).

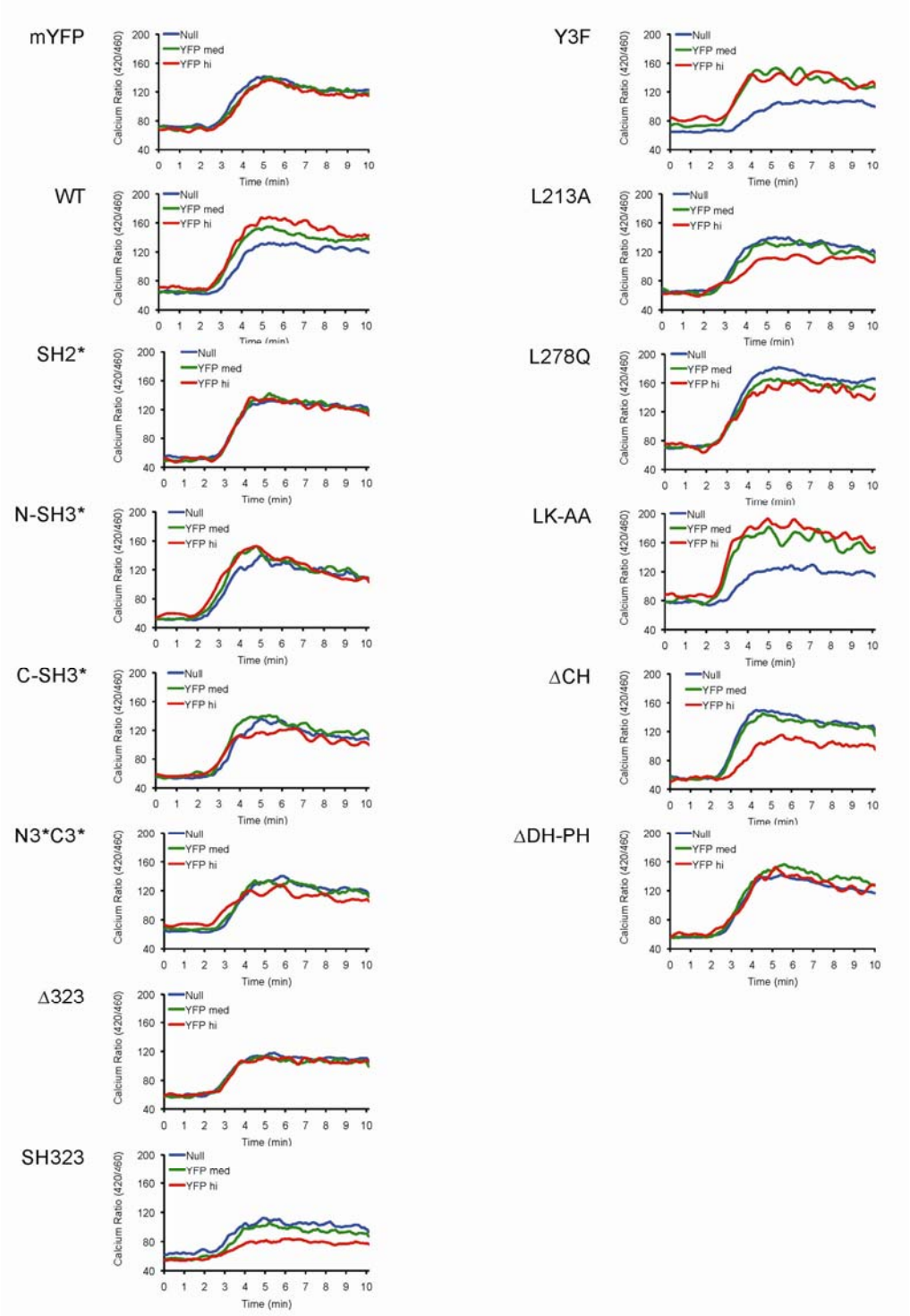

Fig. S1. Effects of Vav1 mutants on TCR-induced Ca^{2+} flux. J.Vav1 cells were transiently transfected with vectors encoding either mYFP or the indicated Vav1-mYFP fusion proteins and were loaded with Indo-1. TCR-induced Ca^{2+} responses were dynamically monitored by flow cytometry. OKT3 (30 ng/ml) was injected after collecting baseline Ca^{2+} signals for 2 min, and ionomycin (1 μM) was injected 10 min later to provide an internal positive control (not shown). For each representative sample shown, smoothed Ca^{2+} traces were generated for subpopulations that contained distinct amounts of mYFP (null, blue traces; moderate, green traces; high, red traces).

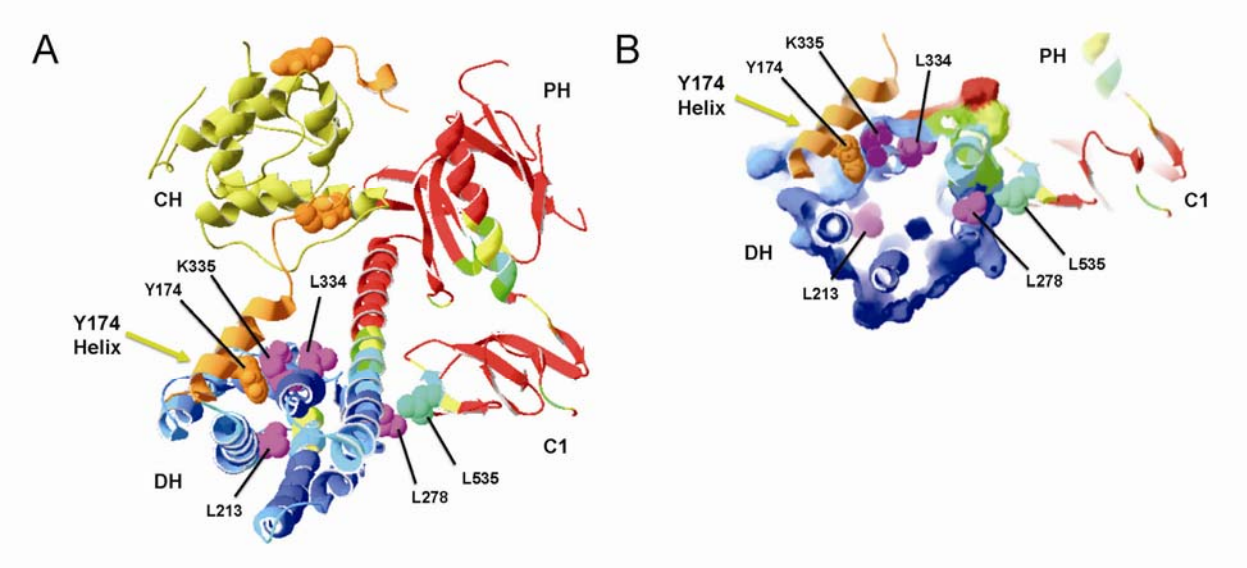

Fig. S2. Mutations that affect the catalytic core of the Vav1 GEF. (**A**) The structure of the auto-inhibited Vav1 N-terminus (3KY9) was fit with the structure of the Rac1-bound DH-PH-C1 module (2VRW) with Swiss-PDBViewer. A ribbon diagram of the auto-inhibited N-terminus of Vav1 is shown, with the CH domain colored yellow, the tyrosine-containing linker colored orange, and the DH-PH-C1 module colored according to the quality of its fit with the Rac1-bound Vav1 (blue for minimal shifts, progressing through green to red for shifts of more than 5 Å). Side-chains of interest are shown as van der Waals surfaces, with DH domain mutants colored purple. (**B**) A molecular surface enclosing the DH domain was added to the representation shown in (A) and colored according to the quality of fit, as described in (A). A cross-section through the DH domain is shown. Of the DH domain mutants examined here, the L213A mutant is expected to alter the packing of the hydrophobic core of the DH domain, the L278Q mutation is likely to perturb the stable interface between the DH domain and the C1 domain (at residue L535), and the L334A/K335A mutation is likely to perturb the auto-inhibited state of the Vav1 N-terminus by eliminating one wall of the pocket into which Y174 packs.

Table S1. Effect of knockdown of Vav1 on SLP-76 microcluster dynamics. J14.SY cells were cotransfected with an empty hairpin expression vector and an mCFP expression vector, or they were cotransfected with a Vav1-specific shRNA expression vector and either an mCFP or Vav1-mCFP expression vector. The Vav1-mCFP vector was rendered insensitive to the shRNA by the introduction of silent point mutations. SLP-76 microcluster behavior was calculated from manual traces of individual microcluster paths from the indicated number of cells.

	Persistence (s)	***P***	**Movement (μm)**	***P***	**Speed (nm/s)**	***P***	**% SLP in clusters**	***P***
Vector/mCFP	202.51 ± 11.29		2.00 ± 0.49		163.30 ± 24.58		56.40 ± 2.76	
shRNA/mCFP	108.05 ± 13.25	**	0.83 ± 0.13	*	136.80 ± 11.63		31.20 ± 4.81	*
shRNA/Vav1	180.76 ± 12.41		2.47 ± 0.46		170.10 ± 21.94		66.60 ± 4.57	

Significant differences from the vector control are indicated with asterisks. *, $P < 0.05$; **, $P < 0.005$.

Table S2. List of primers used to generate the various Vav1 mutations.

Primer	Sequence
SCB045	5`-CTCGCCCTCGCCGGACAC-3`
SCB243	5`-GCCGGGATCCGCCCAGAACAGGGGGATC-3`
SCB244	5`-CATGGCATCCAGGGCCAGCCGCAG-3`
NS705	5`-GATCCGAAGGACTGTACCGGATCA-3`
NS706	5`-TTGAATGATCCGGTACAGTCCTTCG-3`
NS707	5`-TTCAAGAGATGATCCGGTACAGTCCTTCTTTTTGGA-3`
NS708	5`-AGCTTCCAAAAAGAAGGACTGTACCGGATCATCTC-3`
NS723	5`-CATGACAGCAGAAGGCCTCTATCGGATCACAGAG-3`
NS724	5`-CTCTGTGATCCGATAGAGGCCTTCTGCTGTCATG-3`
NS763	5`-GAGTGGGTGGAGACTGAAGTTAGGCCAGC-3`
NS764	5`-GCGCATGAGGTCCTCAAAAATTTCGTCGCCTTCCG-3`
NS765	5`-GCGGAAGGCGACGAAATTTTTGAGGACCTCATGCG-3`
NS766	5’ CCGACCGGTACCTCCATCTTGGGCAGACCCAG
NS767	5’ GCCGCTAGCGCCACCATGGAACTGGGTCTGCCCAAGATGGAG
NS770	5’ CGGATAGATGCAGCAGCGCTTGTCATACTCTGTC
NS771	5’ CGCTGCTGCATCTATCCGGAGAATGCCACCGCC
NS773	5’CGTGTCGTCGATCTGGTCGGACAGGCCTCTGAAGATGTC TTCATCACC
NS774	5’CAGATCGACGACACGGTGGAGGAGGATGAAGACCTGTT TGACTGCGTGGAG
NS830	5’ CAAATACAAGGAGCGCTTCCAGGTCTATGGCCGC
NS831	5’ GCGGCCATAGACCTGGAAGCGCTCCTTGTATTTG
NS832	5’ GATGGTACCTATGCAACGCGTGGCGGCCTATCACCTCCTTCTCCAG
NS833	5’ CTGGAGAAGGAGGTGATAGGCCGCCACGCGTTGCATAGGTACCATC

Supplementary movies

To generate these movies, JV.SC cells were reconstituted with the indicated mYFP-tagged Vav1 fusion proteins (see list below) and stimulated on glass coverslips coated with OKT3 (3 μg/ml). Images were collected over 5 min. SLP-76-mCFP is shown in red and the various Vav-mYFP fusion proteins are shown in green. All movies play at 80 × normal speed. Scale bars represent 10 μm.

Movie S1 and S2: mYFP alone
Movie S3 and S4: Vav1-mYFP
Movie S5: Vav1(SH2*)-mYFP
Movie S6: Vav1(N-SH3*)-mYFP
Movie S7: Vav1(C-SH3*)-mYFP
Movie S8: Vav1(N3*C3*)-mYFP
Movie S9: Vav1(Δ323)-mYFP
Movie S10: Vav1(SH323)-mYFP
Movie S11: Vav1(Y3F)-mYFP
Movie S12: Vav1(L213A)-mYFP
Movie S13: Vav1(L278Q0-mYFP
Movie S14: Vav1(L334A/K335A)-mYFP
Movie S15: Vav1(ΔCH)-mYFP
Movie S16: Vav1(ΔDH-PH)-mYFP